DISCRETE-TIME ANTI-WINDUP: PART 2 - EXTENSION TO THE SAMPLED-DATA CASE

Guido Herrmann[†], Matthew C. Turner[*] and Ian Postlethwaite[‡]

Control and Instrumentation Group, University of Leicester, University Road, Leicester, LE1 7RH, UK
[†] e-mail: gh17@le.ac.uk , [*] e-mail: mct6@le.ac.uk , [‡] e-mail: ixp@le.ac.uk

Keywords: Anti-windup, constrained control, hybrid induced $l_2/\mathcal{L}_2$ norm, sampled-data control

Abstract

The formulation of a discrete-time anti-windup scheme for linear systems with constrained control signals is extended to the sampled-data case. Thus, the control of a continuous-time linear plant via a discrete linear nominal controller and a discrete anti-windup compensator is considered. Stability of the anti-windup compensator is equivalent to the known discrete problem while a hybrid induced $l_2/\mathcal{L}_2$ norm is considered for anti-windup performance. Linear sampled-data lifting techniques are used to reduce the hybrid problem to an optimization problem in the discrete-time domain. A flight control example shows the effectiveness of the discrete and the sampled-data technique.

1 Introduction

For a control system with constrained control signals, anti-windup compensation has become a common technique to prevent destabilization and to retain acceptable performance during saturation, and to enable the system to recover from saturation and to resume nominal control performance. Although there now exist various accounts of continuous-time anti-windup compensation, treatments of discrete anti-windup problems have been less common [1, 2] for which reason the work of [3] considers the discrete counterpart of a continuous-time anti-windup control problem with an $\mathcal{L}_2$-gain requirement for performance [4]. Although some ideas on anti-windup in a sampled-data case are formulated in [5], the strict investigation of anti-windup control *design* problems in a sampled-data frame work has not yet been considered despite the existence of an extensive number of tools for sampled-data analysis of control systems, both for considering linear [6, 7] and non-linear [8, 9] H_∞-control.

Most anti-windup schemes can be parameterized via one single transfer function $M(z)$ such as in [3, 4]. As this can be also done in the sampled-data case, $M(z)$ decouples the anti-windup system into the nominal stable linear sampled-data control loop, a discrete non-linear loop with a dead-zone non-linearity and a linear disturbance filter with discrete input signal and continuous output signal. This shows that the global anti-windup stability problem can be solved for the sampled-data case, as for the discrete-time case, by considering the deadzone function as a sector bounded non-linearity in an LMI-framework. Performance is measured according to the $\mathcal{L}_2$-norm of the linear disturbance filter output in relation to the l_2-norm of a discrete signal entering the discrete non-linear loop. This resembles the case of [3] where the respective l_2-gain has been minimized. In the case of the sampled-data anti-windup system, linear sampled-data lifting methods [6] are used to convert the linear disturbance filter from a hybrid filter with discrete-time input and continuous-time output to a discrete-time filter. This filter then has an l_2-output norm of the same value as the $\mathcal{L}_2$-norm of the output signal of the hybrid filter. This approach allows one to consider an anti-windup problem in the discrete-time domain as in [3]. Hence in this approach, the linear features of the sampled-data anti-windup scheme are fully exploited preventing the complexity of non-linear sampled-data analysis.

This article introduces at first a sampled-data control anti-windup problem to which linear lifting techniques are applied thereafter. Then, several anti-windup controller configurations are considered which are finally exemplified for a non-trivial flight control example in comparison to the discrete-time anti-windup technique of [3].

2 The sampled-data anti-windup problem

The sampled-data system of Figure 1 shows from a stability and a performance point of view the equivalence of a control signal constrained system considering control signal constraints before the continuous-time linear plant, inside the discrete controller or at both points. The schematic of Figure 1 clarifies that it is permissible to consider the anti-windup compensation in terms of a generic anti-windup scheme as we did in [3]. The sampled-data system from Figure (1) consists of a

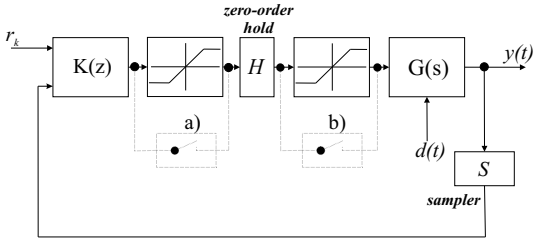

Figure 1: Sampled-data control system with constrained control input: Case a) switch (a) closed, Case b) switch (b) closed, Case c) all switches open

continuous-time linear stable plant $G(s)$ with detectable states $x_p(t) \in \mathbb{R}^{n_p}$

$$G(s) \sim \left\{ \begin{array}{rcl} \dot{x}_p(t) & = & A_p x_p(t) + B_p u_m(t) + B_{pd} d(t) \\ y(t) & = & C_p x_p(t) + D_p u_m(t) + D_{pd} d(t) \end{array} \right. \quad (1)$$

where $u_m(t) \in \mathbb{R}^m$ is the actual control input to the plant, $d(t) \in \mathbb{R}^{n_d}$ is some disturbance and $y(k) \in \mathbb{R}^q$ is the measured output so that

$$G_1(s) \sim (A_p, B_{pd}, C_p, D_{pd}),\ G_2(s) \sim (A_p, B_p, C_p, D_p). \quad (2)$$

For this plant, a discrete nominal controller $K(z) = [K_1(z)\ K_2(z)]$, $y_c = K_1(z)y + K_2(z)r$, has been designed:

$$K(z) \sim \left\{ \begin{array}{rcl} x_c(k+1) & = & A_c x_c(k) + B_c y(k) + B_{cr} r(k) \\ y_c(k) & = & C_c x_c(k) + D_c y(k) + D_{cr} r(k) \end{array} \right. \quad (3)$$

so that poles of $(I - K_2(z)G_2(z))^{-1}$ are in the open unit disk and $\lim_{z\to\infty}(I - K_2(z)G_2(z))^{-1}$ exists where $x_c(k) \in \mathbb{R}^{n_c}$ is the controller state, $y_c(k) \in \mathbb{R}^m$ is the desired controller output, $r(k) \in \mathbb{R}^{n_r}$ is the reference command and $G_2(z) =$

$H_\tau G_2(s) S_\tau$ is the zero-order-hold of $G_2(s)$. The discrete controller acts according to some nominal stability and performance criteria which have been determined for the control system without the occurrence of saturation. The saturation function is defined as

$$\mathrm{sat}(u) := [\mathrm{sat}_1(u_1), \ldots, \mathrm{sat}_m(u_m))] \tag{4}$$

where $\mathrm{sat}_i(u_i) := \mathrm{sign}(u_i) \times \min\{|u_i|, \bar{u}_i\}$ and $\bar{u}_i > 0$. The connection between the continuous-time plant $G(s)$ and the discrete controller $K(z)$ is provided via the sample element S_τ:

$$v = S_\tau y \;\Leftrightarrow\; v(i) = y(k\tau),\ k = 0, 1, 2, 3..., \ \tau > 0, \tag{5}$$

defining, from a continuous-time signal $y(t)$, a discrete-time output vector $\mathbf{v}(k)$ for constant sampling-time τ. In contrast, the hold element H_τ is the operator:

$$u_m = H_\tau z \Leftrightarrow \forall t \in [k\tau, (k+1)\tau) :\ u_m(t) = z(k),\ k = 0, 1, ... \tag{6}$$

which converts a discrete-time series $z(k)$ into a continuous step-function $u_m(t)$ using a constant sampling-time τ.

It is readily understood from the sampled-data system of Figure 1 that the closed-loop system's stability and input-to-output performance from the relevant exogenous inputs $d(t)$, $r(k)$ to the measured output $y(t)$ is for all three cases (a), (b) and (c) equivalent due to the particular linear characteristic of the operator H_τ. This allows us to deal with the saturation non-linearity via the generic conditioning scheme of Figure 2 involving the

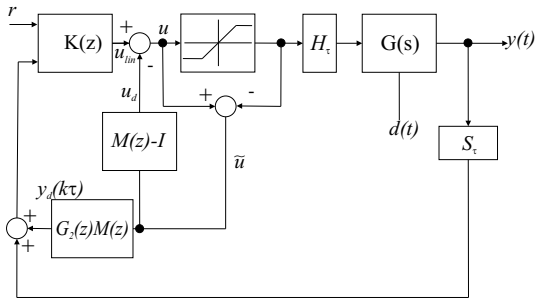

Figure 2: Anti-windup scheme: Conditioning via $M(z)$

transfer function $M(z)$ as considered for the discrete case in [3]. It is readily understood using the linear super-position principle that this anti-windup scheme is equivalent to the configuration of Figure 3 in terms of stability and input-to-output behaviour, where the non-linear element is the dead-zone non-linearity satisfying:

$$\mathrm{Dz}(u) = u - \mathrm{sat}(u). \tag{7}$$

Hence, stability of the anti-windup compensator has been reduced to a discrete stability problem (the nonlinear loop involves purely discrete elements), while the actual anti-windup problem of interest, that is the induced norm from $u_{lin}(k)$ to $y_d(t)$ (which involves a mixture of discrete and continuous elements), for this configuration is defined as follows:

Definition 1 *The anti-windup compensator $M(z)$ is said to solve strongly the anti-windup problem if the closed loop system in Figure 3 is internally stable and well-posed and if*

1. $\mathrm{dist}(u_{lin}, \mathcal{U}) = 0, \quad \forall t \geq 0$ *then* $y_d = 0, \quad \forall t \geq 0$ *(assuming zero initial conditions for the anti-windup compensator and* $\mathcal{U} := [-\bar{u}_1, \bar{u}_1] \times, \ldots, \times [-\bar{u}_m, \bar{u}_m]$*).*

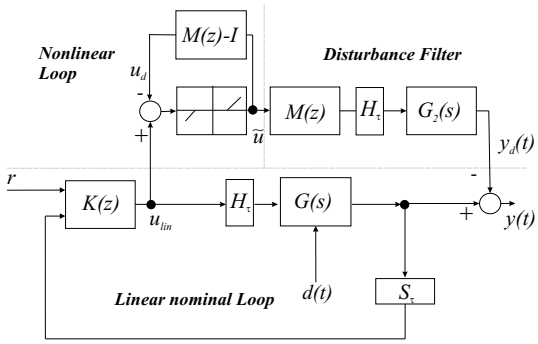

Figure 3: Equivalent representation for the $M(z)$ conditioned anti-windup scheme

2. *The operator $\mathcal{T} : u_{lin} \mapsto y_d$ is well-defined and has a finite induced $l_2/\mathcal{L}_2$-norm:*

$$\exists \gamma :\ \|\mathcal{T}\|_{l_2/\mathcal{L}_2} = \gamma = \sup_{u_{lin} \neq 0} \frac{\sqrt{\int_0^\infty \|y_d(t)\|^2 \, dt}}{\sqrt{\sum_{k=0}^\infty \|u_{lin}(k)\|^2}} \tag{8}$$

Hence, this sampled-data anti-windup problem involves the computation of a hybrid induced norm. In [3], the discrete anti-windup problem has been solved by considering the linear plant and controller characteristics while the saturation/deadzone non-linearity had been expressed in terms of a sector non-linearity. This frame-work can be used here also by incorporating the theoretical frame-work of lifting in sampled-data systems from [6]. For this, the theoretical background is explained next. In particular, the $\mathcal{L}_2$-norm of the output of the operator $G_2(s)H_\tau$ is of interest for us for computation of the $\mathcal{L}_2$-norm of $y_d(t)$.

3 Sampled-data lifting techniques in application to the anti-windup problem

From Section 2, the sampled-data system of interest for us operates in two different domains, in the space of Lebesgue integrable continuous vector valued functions $\mathfrak{C}$ and in the space of vector valued sequences $\mathfrak{S}$, considering an appropriately dimensioned Eucledian vector space $\mathcal{E}$, e.g. $\mathcal{E} = \mathbb{R}^q$. The two spaces, $\mathfrak{C}$ and $\mathfrak{S}$, are joined via the sample-operator S_τ (5) and the zero-order hold H_τ (6). Thus, the sample element S_τ and the hold H_τ element are operators satisfying:

$$S_\tau : \mathfrak{C} \to \mathfrak{S},\ H_\tau : \mathfrak{S} \to \mathfrak{C}.$$

For analysis of the $\mathcal{L}_2$-characteristics of $G_2(s)H_\tau$, it is shown at first that a continuous-time signal can be lifted into a discrete-time representation where in particular the respective inner product and l_2-norm follow the same rules and have the same value as for their continuous-time counterpart [6]: Suppose that for $y(t) \in \mathfrak{C}$ the $\mathcal{L}_2$-integral is finite:

$$y(t) \in \mathcal{L}_2(\mathbb{R}, \mathcal{E}) :\ \int_0^\infty y'(t) y(t) dt < \infty,$$

while the inner product of $y(t),\ z(t) \in \mathcal{L}_2(\mathbb{R}, \mathcal{E})$ is

$$< y(t), z(t) >_{\mathcal{L}} = \int_0^\infty y(t) z(t) dt$$

Then consider

$$y(k)(t) \stackrel{def}{=} y(k\tau + t),\ 0 \leq t < \tau$$

so that each element $y(k)(t) \in \mathcal{K}$ where $\mathcal{K} = \mathcal{L}_2([0,\tau),\mathcal{E})$. An inner product $< \cdot >_{\mathcal{K}}$ is defined by:

$$< y(k)(t), z(k)(t) >_{\mathcal{K}} = \int_0^\tau (y(k)(t))' z(k)(t) dt, \quad (9)$$

This procedure creates a discrete-time signal $\underline{y}$ in the space $l_2(\mathbb{Z},\mathcal{K})$ via a lifting operator L:

$$Ly = \underline{y} = \begin{bmatrix} y(0)(t) \\ y(1)(t) \\ y(2)(t) \\ \vdots \end{bmatrix} \quad (10)$$

with inner product:

$$< \underline{y}, \underline{z} >_l = \sum_{k=0}^{\infty} < y(k), z(k) >_{\mathcal{K}}$$

which implies that the operator L preserves the inner product $< y, z >_l = < Ly, Lz >_{\mathcal{L}}$ and respectively the $\mathcal{L}_2$-norm on the infinite horizon defined via the inner product.

The L-operator allows one to eliminate the continuous/discrete-time anti-windup problem by creating an overall discrete system. Hence, we may now consider the operator $LG_2(s)H_\tau$, where the continuous-time linear time-invariant system $G_2(s)$ is:

$$G_2(s) \sim \left\{ \begin{array}{rcl} \dot{x}_2(t) & = & A_p x_2(t) + B_p u_2(t) \\ y_d(t) & = & C_p x_2(t) + D_p u_2(t) \end{array} \right.$$

with state-vector $x_2(t) \in \mathfrak{C}$. By [6], it can be shown that the discrete operator LG_2H_τ from $\mathcal{L}_2(\mathbb{R},\mathcal{E})$ to $l_2(\mathbb{Z},\mathcal{K})$ has the following state space representation with initial state $\boldsymbol{x}_2(k=0) = x_2(t=0)$ and $u_2 = H_\tau \boldsymbol{u}_2(k)$:

$$LG_2H_\tau \sim \left\{ \begin{array}{rcl} \boldsymbol{x}_2(k+1) & = & A_d \boldsymbol{x}_2(k) + B_d \boldsymbol{u}_2(k) \\ y_d(k)(t) & = & (\underline{C}\boldsymbol{x}(k))(t) + (\underline{D}\boldsymbol{u}_2(k))(t) \end{array} \right. ,$$

where the matrices $A_d = e^{\tau A_p}$ and $B_d = \int_0^\tau e^{tA_p} dt B_p$ are linear operators between two finite dimensional Eucledian vector spaces, while $\underline{C}$ and $\underline{D}$ are operators with a vector space as argument space and $\mathcal{K}$ as object space:

$$\begin{array}{rcl} (\underline{C}\boldsymbol{x}_2(k))(t) & := & C_p e^{tA_p} \boldsymbol{x}_2(k), \\ (\underline{D}\boldsymbol{u}_2(k))(t) & := & \left[D_p + \int_0^t C_p e^{sA_p} ds B_p \right] \boldsymbol{u}_2(k). \end{array}$$

3.1 The l_2-norm of the output of the operator LG_2H_τ

Using the lifting approach, the $\mathcal{L}_2$-norm of the output signals GH_τ is conveniently calculated by computing the l_2-norm of the output signal of LG_2H_τ. Note that $G_2(s)$ is stable and consider $\boldsymbol{u}_2 = (\boldsymbol{u}_2(k),\ k = 0,1,2,...)$

$$\boldsymbol{u}_2 \in l_2(\mathbb{Z},\mathcal{E}) : \ \sum_{k=0}^{\infty} (\boldsymbol{u}_2(k))' \boldsymbol{u}_2(k) < \infty$$

for $\underline{y}_d = LG_2(s)H_\tau \mathbf{u}$, $\underline{y}_d \in l_2(\mathbb{Z},\mathcal{K})$ with state vector $x_2(k)$ at time instant k. We know that

$$\int_0^\infty y_d'(t) y_d(t) dt = \sum_{k=0}^{\infty} < y_d(k)(t), y_d(k)(t) >_{\mathcal{K}}$$

while using the notation of (10) and (9) it follows:

$$\begin{array}{l} < y_d(k)(t), y_d(k)(t) >_{\mathcal{K}} = \int_0^\tau (C_p e^{lA_p} \boldsymbol{x}_2(k) + [D_p + \int_0^l C_p e^{sA_p} ds B_p] \boldsymbol{u}_2(k))' \times \\ \quad (C_p e^{lA_p} \boldsymbol{x}_2(k) + [D_p + \int_0^l C_p e^{sA_p} ds B_p] \boldsymbol{u}_2(k)) dl \\ \quad = \begin{bmatrix} \boldsymbol{x}_2(k) \\ \boldsymbol{u}_2(k) \end{bmatrix}' \mathbf{U} \begin{bmatrix} \boldsymbol{x}_2(k) \\ \boldsymbol{u}_2(k) \end{bmatrix} \end{array}$$

where

$$\mathbf{U} = \begin{bmatrix} \tilde{Z}_1 & \tilde{Z}_2' B_p + (e^{\tau A_p'} - I)(A_p^{-1})' C_p' (D_p - C_p A_p^{-1} B_p) \\ * & \mathbf{U}_3 \end{bmatrix},$$

$$\begin{array}{l} \mathbf{U}_3 = B_p' \tilde{Z}_3 B_p + \tau D_p' D_p - \tau D_p' C_p A_p^{-1} B_p - \tau B_p' (A_p^{-1})' C_p' D_p \\ + \tau B_p' (A_p^{-1})' C_p' C_p A_p^{-1} B_p + D_p' C_p A_p^{-2} (e^{\tau A_p} - I) B_p \\ + B_p' (e^{\tau A_p'} - I)(A_p^{-2})' C_p' D_p - B_p' (e^{\tau A_p'} - I)(A_p^{-2})' C_p' C_p A_p^{-1} B_p \\ - B_p' (A_p^{-1})' C_p' C_p A_p^{-2} (e^{\tau A_p} - I) B_p \end{array} \quad (11)$$

and

$$\begin{array}{l} \tilde{Z}_1 = \int_0^\tau \underbrace{e^{lA_p'} C_p' C_p e^{lA_p}}_{Z_1(l)} dl, \ \tilde{Z}_2 = \int_0^\tau \underbrace{e^{lA_p'} (A_p^{-1})' C_p' C_p e^{lA_p}}_{Z_2(l)} dl, \\ \tilde{Z}_3 = \int_0^\tau \underbrace{e^{lA_p'} (A_p^{-1})' C_p' C_p A_p^{-1} e^{lA_p}}_{Z_3(l)} dl. \end{array} \quad (12)$$

Remark 1 The integrals (12) of type $\int_0^\tau e^{lA_p'} X e^{lA_p} dl$ for appropriately dimensioned matrix X are readily computed: From [10], the matrix function $Z(t)$

$$Z(t) = e^{tA_p'} X e^{tA_p}$$

is the solution for

$$\frac{dZ(t)}{dt} = A_p' Z + Z A_p, \ \ Z(t=0) = X.$$

Hence, given $Z(\tau)$, $Z(0)$, A_p, the integral $\int_0^\tau Z(t) dt$ can be calculated via the following Lyapunov equation:

$$Z(\tau) - Z(0) = A_p' \int_0^\tau Z(t) dt + \int_0^\tau Z(t) dt A_p. \quad (13)$$

Hence, employing $Z_i(l)$, $i = 1,2,3$, from (12), the Lyapunov equation of (13) can be used to derive the values of $\tilde{Z}_i$. ∘

It is now possible to define a discrete system $\tilde{y}_d = \tilde{G}_2(z)\boldsymbol{u}_2$ for $\boldsymbol{x}_2(k=0) = x_2(t=0)$:

$$\tilde{G}_2(z) \sim \left\{ \begin{array}{rcl} \boldsymbol{x}_2(k+1) & = & A_d \boldsymbol{x}_2(k) + B_d \boldsymbol{u}_2(k) \\ \tilde{y}_d(k) & = & \tilde{C}\boldsymbol{x}_2(k) + \tilde{D}\boldsymbol{u}_2(k) \end{array} \right. ,$$

where

$$\mathbf{U} = \begin{bmatrix} \tilde{C} & \tilde{D} \end{bmatrix}' \begin{bmatrix} \tilde{C} & \tilde{D} \end{bmatrix}.$$

for which

$$\sum_{k=0}^{\infty} \tilde{y}_d'(k) \tilde{y}_d(k) = \sum_{k=0}^{\infty} < y_d(k)(t), y_d(k)(t) >_{\mathcal{K}} = \int_0^\infty y_d'(t) y_d(t) dt.$$

Note that the output dimension of $\tilde{G}_2(z)$ is not necessarily similar to the one of the output $G_2(s)H_\tau$. Since the l_2-norm of the output signal of $\tilde{G}_2(z)$ is of the same value as the $\mathcal{L}_2$-norm of $G_2(s)H_\tau$ for given $\boldsymbol{u}_2$ and initial state $\boldsymbol{x}_2(k=0) = x_2(t=0)$, it is now readily used in the anti-windup analysis as depicted in Figure 4 for optimization of the induced $l_2/\mathcal{L}_2$-norm, which is the induced l_2-norm from u_{lin} to $\tilde{y}_d$.

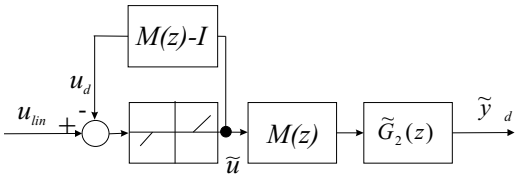

Figure 4: Equivalent configuration of the strong, $M(z)$-conditioned sampled-data anti-windup problem

4 Full order anti-windup synthesis

As in [3], an anti-windup controller with the same order as $G_2(z)$ may be termed a full order compensator. From Section 2 and [3], it is understood that the choice $M(z) = I$ provides an anti-windup compensator which solves strongly the anti-windup problem of Definition 1 as it recovers the internal model control scheme. Hence, also for the sampled-data anti-windup problem, there always exists a full-order anti-windup compensator.

For minimization of $\|\mathcal{T}\|_{l_2/\mathcal{L}_2}$, the artificial plant $\tilde{G}_2(z)$ may be expressed in terms of its right coprime factorization $\tilde{G}_2(z) = N(z)M(z)^{-1}$ for which we choose $N(z)$ and $M(z)$ to have the same state-space as $\tilde{G}_2(z)$. Hence, as in [3] choose:

$$\begin{aligned} \boldsymbol{x}_2(k+1) &= (A_d + B_d F)\boldsymbol{x}_2(k) + B_d\tilde{u}(k) && (14)\\ u_d(k) &= F\boldsymbol{x}_2(k) && (15)\\ \tilde{y}_d(k) &= (\tilde{C} + \tilde{D}F)\boldsymbol{x}_2(k) + \tilde{D}\tilde{u}(k) && (16) \end{aligned}$$

where $\tilde{u}(k) = Dz(u_{lin}(k) - u_d(k))$. Hence, as in [3], the l_2-gain for the input-output u_{lin} to $\tilde{y}_d$ can be minimized for the parameter F using the following Theorem:

Theorem 1 *There exists a dynamic compensator $M(z)$ of order n_p which solves strongly the anti-windup problem if there exist matrices $Q > 0, W = \mathrm{diag}(\mu_1, \ldots \mu_m) > 0, L \in \mathbb{R}^{(m+q)\times m}$ and a scalar $\mu > 0$ such that the following linear matrix inequality (LMI) is satisfied*

$$\begin{bmatrix} -Q & -L' & 0 & Q\tilde{C}+L'\tilde{D}' & QA_d+L'B_d' \\ \star & -2U & I & U\tilde{D}' & UB_d' \\ \star & \star & -\mu I & 0 & 0 \\ \star & \star & \star & -I & 0 \\ \star & \star & \star & \star & -Q \end{bmatrix} < 0 \quad (17)$$

Furthermore, if this inequality is satisfied, a suitable F for (14)-(16) achieving $\|\mathcal{T}\|_{l_2/\mathcal{L}_2} < \gamma = \sqrt{\mu}$, is given by $F = LQ^{-1}$.

The proof of this theorem readily follows from the proof of Theorem 1 in [3].

5 Static anti-windup synthesis

As for [3], in practice it is not desirable to increase the controller order from n_c to $n_c + n_p$ to compensate for the case of saturation. It seems to be more suitable to keep the anti-windup compensator as simple as possible for which the easiest choice are static matrix elements Θ_1 and Θ_2 (instead of the dynamic elements $M(z) - I$ and $G_2(z)M(z)$) as depicted in Figure 5. From Figure 2 and 5 using the same approach as in [3], both

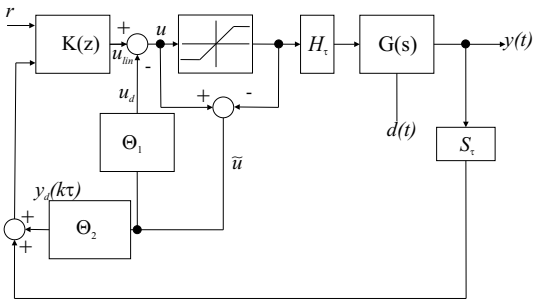

Figure 5: Static anti-windup configuration

schemes are equivalent if

$$M = (I - K_2(z)G_2(z))^{-1}(-K_2(z)\Theta_2 + \Theta_1 + I). \quad (18)$$

Considering (18), a state space representation for the transfer $M(z) - I$ and $\tilde{G}_2(z)M(z)$ is given by:

$$\begin{bmatrix} M(z)-I \\ \tilde{G}_2(z)M(z) \end{bmatrix} \sim \begin{cases} \bar{x}(k+1) = \bar{A}\bar{x}(k) + (B_0 + \bar{B}\Theta)\tilde{u}(k) \\ u_d(k) = \bar{C}_1\bar{x}(k) + (D_{01} + \bar{D}_1\Theta)\tilde{u}(k) \\ \tilde{y}_d(k) = \bar{C}_2\bar{x}(k) + (\tilde{D}_{02} + \tilde{D}_2\Theta)\tilde{u}(k) \end{cases} \quad (19)$$

and $\Theta = [\Theta_1' \Theta_2']'$ for which a minimal realization is presented in the Appendix. In this sense, a sub-optimal result for the static anti-windup compensator is readily obtained from [3]:

Theorem 2 *There exists a static compensator $\Theta = [\Theta_1' \Theta_2']' \in \mathbb{R}^{(m+q)\times m}$ which solves strongly the anti-windup problem if there exist matrices $Q > 0, U = \mathrm{diag}(\mu_1, \ldots, \mu_m) > 0, L \in \mathbb{R}^{(m+q)\times m}$ and a postive real scaler $\mu > 0$ such that the following LMI is satisfied*

$$\begin{bmatrix} -Q & -Q\bar{C}_1' & 0 & Q\bar{C}_2' & Q\bar{A}' \\ \star & -2U - D_{01}U - \bar{D}_1L - UD_{01}' - L'\bar{D}_1' & I & U\tilde{D}_{02}' + L'\tilde{D}_2' & UB_0 + L'\bar{B}' \\ \star & \star & -\mu I & 0 & 0 \\ \star & \star & \star & -I & 0 \\ \star & \star & \star & \star & -Q \end{bmatrix} < 0 \quad (20)$$

Furthermore, if this inequality is satisfied a suitable Θ achieving $\|\mathcal{T}\|_{l_2/\mathcal{L}_2} < \gamma = \sqrt{\mu}$ is given by $\Theta = LU^{-1}$.

Remark 2 Note that the low order anti-windup compensator and well-posedness of all the anti-windup schemes can be discussed as in [3]. ◦

6 Case study: high α aircraft

To demonstrate a comparative analysis of our results, we study a simple model of a high α aircraft, linearised at a high angle-of-attack (α) [11, eqn. A2-A4]. This is an interesting model to study, partly due to the poor performance it exhibits under saturation constraints on the control magnitude and partly due to the highly coupled system characteristics which makes this plant an ideal test-bed for multivariable anti-windup techniques.

For our study, we used the first design approach of [11], an $\mathcal{H}_\infty$ mixed sensitivity design from Figure 2 and equation (19)-(21) of [11]. To obtain from the continuous design problem a

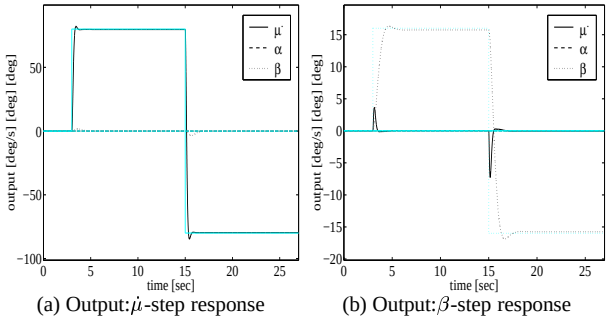

(a) Output:$\dot{\mu}$-step response (b) Output:β-step response

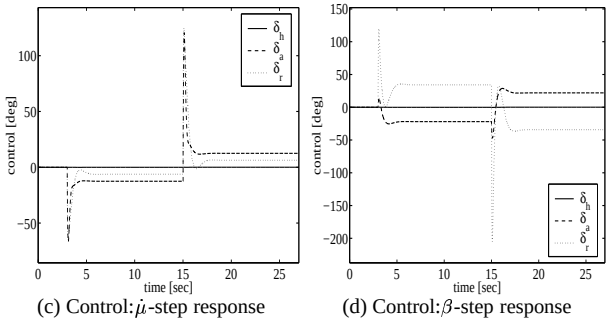

(c) Control:$\dot{\mu}$-step response (d) Control:β-step response

Figure 6: Step response for $\dot{\mu}$, β without saturation constraints for $\tau = 10$ms; light=demand, black=data

discrete problem, it has been zero-order hold discretized which ensures the design of a stable controller for *any* sampling time τ. For our work, we considered a sampling time $\tau = 10$ ms as stated in [11] and the significantly higher sampling time of $\tau = 1.3$ sec. The higher sampling time is only of academic interest to show the characteristics of the sampled-data anti-windup technique as opposed to the discrete anti-windup technique of [3]. In contrast to [11], we did not attempt any order reduction, yielding a nominal controller order of 12. The controlled variables are $\dot{\mu}, \alpha, \beta$ which represent the stability-axis roll rate, the angle-of-attack and the side-slip angle, respectively. The plant inputs are $\delta_h, \delta_a, \delta_r$ which represent the elevator deflection, the aileron deflection and the rudder deflection respectively. These actuators are subject to the following constraints: $|\delta_h| \leq 25^o$, $|\delta_a| \leq 20^o$ and $|\delta_r| \leq 30^o$.

Considering the control performance for $\tau = 10$ ms first, Figure 6 shows the response of the high-α aircraft to demands in the $\dot{\mu}$ and β channels without saturation constraints showing a high actuator activity in most of the control channels. This indicates a significant amount of coupling. (Due to space reasons, channel α is not considered.) Figure 7 shows the response of the high-α aircraft when the saturation constraints are imposed on the control signal for the same demands as those used for the unconstrained responses. In particular for $\tau = 10$ ms, the performance has deteriorated in both channels. The demand in $\dot{\mu}$ causes the aircraft to lose virtually all its tracking ability in the $\dot{\mu}$ channel; the demand in β gives rise to a highly coupled and oscillatory type of behaviour. In order to improve the response of the system, a full-order anti-windup compensator was synthesised using the LMI in Theorems 1 from [3] and from this paper. This yielded an optimal value of $\gamma \approx 5.729$ ($\tau = 10$ ms) for the discrete and $\gamma \approx 5.727 \times \sqrt{\tau}$ for the sampled-data anti-windup optimization. Both, the discrete and the sampled-data anti-windup optimization result, show identical performance results as presented in Figure 8. Hence, the aircraft responses have been dramatically improved. For the demand on $\dot{\mu}$, the tracking performance has been tightened considerably; for the demand on β, apart from an initial period, the coupling has been eliminated and the oscillatory response damped, compared to the response without using anti-

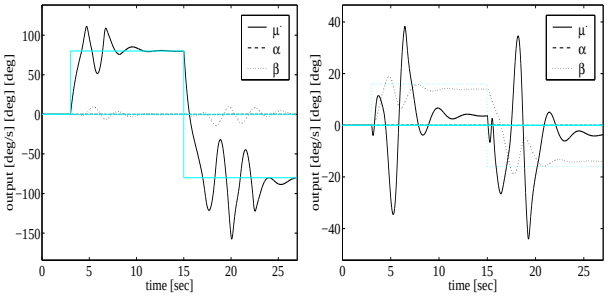

(a) Output:$\dot{\mu}$-step response (b) Output:β-step response

Figure 7: Step response for $\dot{\mu}$, β with control constraints for $\tau = 10$ms; light=demand, black=data

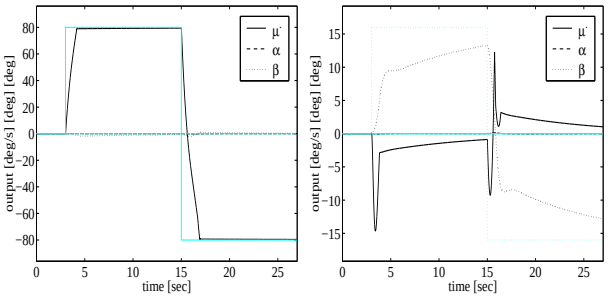

(a) Output:$\dot{\mu}$-step response (b) Output:β-step response

Figure 8: Step response for $\dot{\mu}$ and β with full order anti-windup for $\tau = 10$ms, light=demand, black=data

windup. On the negative side, the anti-windup compensator does slow down the tracking performance in this channel. The main problem with full-order anti-windup is that it requires a significant amount of extra on-line computation to implement. Static-anti-windup, although not guaranteed to be feasible can be an alternative to this. For this plant and controller combination static anti-windup was indeed feasible and, using Theorems 2 from [3] and from this paper, resulted in a $\gamma \approx 6.814$ ($\tau = 10$ ms) for the discrete and $\gamma = 6.812 \times \sqrt{\tau}$ for the sampled-data technique, where both optimization approaches show again the same performance result as depicted in Figure 9. For the demand on $\dot{\mu}$, the response is almost identical to that of the full-order anti-windup compensator. For the demand in β, we can again see that the coupling has been improved, except for a sharp initial peak. In fact, the tracking performance of the compensator seems somewhat better than for the full order case, with a sharper response in β. It was also possible to obtain some good low order response, although space prohibits

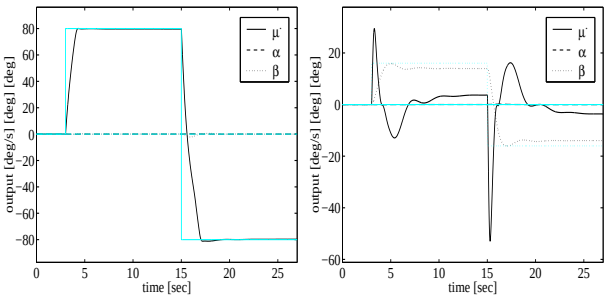

(a) Output:$\dot{\mu}$-step response (b) Output:β-step response

Figure 9: Step response for $\dot{\mu}$ and β with static anti-windup for $\tau = 10$ms, light=demand, black=data

a discussion of these.

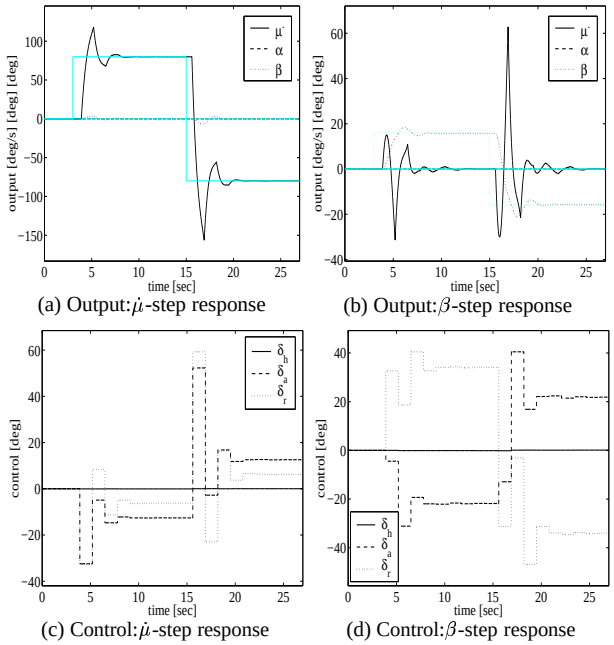

(a) Output:$\dot{\mu}$-step response (b) Output:β-step response

(c) Control:$\dot{\mu}$-step response (d) Control:β-step response

Figure 10: Step response for $\dot{\mu}$, β without saturation constraints for $\tau = 1300$ ms, light=discrete AW, black=sampled-data AW

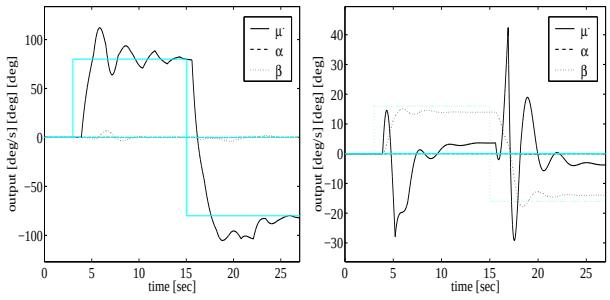

(a) Output:$\dot{\mu}$-step response (b) Output:β-step response

Figure 11: Step response for $\dot{\mu}$, β with control constraints, $\tau = 1300$ ms, light=discrete AW, black=sampled-data AW

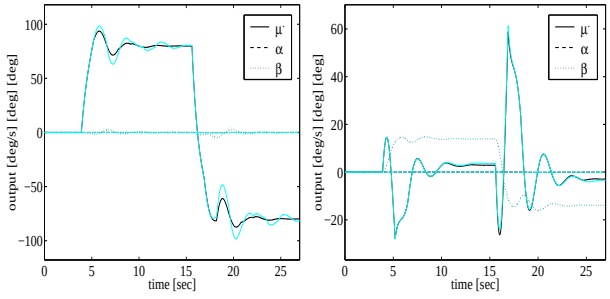

(a) Output:$\dot{\mu}$-step response (b) Output:β-step response

Figure 12: Step response for $\dot{\mu}$ and β with full order anti-windup for $\tau = 1300$ms, light=discrete AW, black=sampled-data AW

In most of our examples, we have found that the discrete approach and the sampled-data approach to performance optimization show very similar results. Only for a very large sampling time of $\tau = 1.3$ sec, we observed an advantage of the sampled-data technique over the discrete optimization approach. The nominal behaviour of the controller without any anti-windup compensation is shown in Figures 10 and 11 for control without and with control signal constraints respectively. A full-order anti-windup optimization according to Theorems 1 from [3] and from this paper, gives the respective results of $\gamma = 5.727$ and $\gamma = 5.727 \times \sqrt{\tau}$. The discrete anti-windup approach does not seem to improve the nominal control behaviour as presented in Figures 11 and 12. The sampled-data techniques provides largely similar results where, in contrast to the discrete approach, the settling behaviour in the $\dot{\mu}$-channel appears to be improved. It is believed that significant research has to be invested in this issue considering also other plants with rich high frequency system dynamics.

7 Conclusions

This paper has provided an extension of a novel approach to anti-windup compensator design from discrete to sampled-data compensator optimization. The theoretical frame-work considers linear sampled-data lifting techniques to derive a solution for the overall nonlinear anti-windup problem. An example shows that both anti-windup compensator design approaches are effective while the sampled-data technique shows some advantage for a Nyquist frequency significantly smaller than the maximal frequency range of the plant dynamics.

A The state space representation for the static anti-windup scheme

Considering all the notation from the Sections 3 and 5 and using the fact that $G_2(z) \equiv (A_d, B_d, C_p, D_p)$ it follows for (19) and $\Delta := (I - D_p D_c)^{-1}$, $\tilde{\Delta} := (I - D_c D_p)^{-1}$ that:

$$\bar{A} = \begin{bmatrix} A_d + B_d\tilde{\Delta}D_c & B_d\tilde{\Delta}C_c \\ B_c\Delta C_p & A_c + B_c\Delta D_p C_c \end{bmatrix}, B_0 = \begin{bmatrix} B_d\tilde{\Delta} \\ B_c\Delta D_p \end{bmatrix}, \bar{B} = \begin{bmatrix} B_d\tilde{\Delta} & -B_d\tilde{\Delta}D_c \\ B_c\Delta D_p & -B_c\Delta \end{bmatrix}$$

$$\bar{C}_1 = \begin{bmatrix} \tilde{\Delta}D_c C_p & \tilde{\Delta}C_c \end{bmatrix}, D_{01} = \tilde{\Delta}D_c D_p, \bar{D}_1 = \begin{bmatrix} I + \tilde{\Delta}D_c D_p & -\tilde{\Delta}D_c \end{bmatrix}$$

$$\tilde{C}_2 = \begin{bmatrix} \tilde{C} + \tilde{D}\tilde{\Delta}D_c C_p & \tilde{D}\tilde{\Delta}C_c \end{bmatrix}, \tilde{D}_{02} = (\tilde{D} + \tilde{D}\tilde{\Delta}D_c D_p), \quad \tilde{D}_2 = \begin{bmatrix} \tilde{D} + \tilde{D}\tilde{\Delta}D_c D_p & -\tilde{D}\tilde{\Delta}D_c \end{bmatrix}.$$

References

[1] K.S. Walgama and J. Sternby. Conditioning technique for multi-input multioutput processes with input saturation. *IEE Proc. D*, 140(4):231–241, 1993.

[2] M. Soroush, N. Mehranbod, and S. Mehdi-Alaie. Directionality in input-constrained systems: its defi nition and optimal compensation. *Proc. Amer. Cont. Conf.*, pp. 2002–2006, 1999.

[3] M. C. Turner, G. Herrmann, and I. Postlethwaite. Discrete-time anti-windup: Part 1 - stability and performance. In *Proc. ECC2003, Cambridge*.

[4] M.C. Turner and I. Postlethwaite. A new perspective on static and low order anti-windup synthesis. *submitted for journal publ.*, 2001.

[5] A. Bemporad, A. Teel, and L. Zaccarian. $\mathcal{L}_2$ Anti-windup via Receding Horizon Optimal Control. *Proc. Amer. Cont. Conf.*, 2002.

[6] T. Chen and B. Francis. *Optimal Sampled-Data Control Systems*. Springer-Verlag, London, 1995.

[7] B. A. Bamieh and J. B. Pearson. A general framework for linear periodic systems with applications to H_∞-sampled-data systems. *IEEE Trans. Aut. Cont.*, 37:418–435, 1992.

[8] L. Zaccarian, A. R. Teel, and D. Nešić. On fi nite gain L_p-gain stability of nonlinear sampled-data systems. In *Proc. Amer. Cont. Conf., Anchorage*, pp. 3523–3528, 2002.

[9] G. Herrmann, S. K. Spurgeon, and C. Edwards. Discretization of a non-linear, exponentially stabilizing control law using an L_p-gain approach. In *Proc. 39th Conf. on Dec. & Cont., Sydney*, pp. 3398–3403, 2000.

[10] P. Lancaster and M. Tismenetsky. *The Theory of Matrices*. Ac. Press, Orlando, 2nd ed., 1985.

[11] J.-S. Yee, J.L. Wang, and Sundararajan. Robust sampled data $\mathcal{H}_\infty$ flight controller design for high α stability-axis roll manoeuver. *Cont. Engin. Pract.*, 8:735–747, 2001.